Proc. Natl. Acad. Sci. USA
Vol. 95, pp. 6590–6595, June 1998
Engineering

Microvascular and tissue oxygen gradients in the rat mesentery

(arterioles/vessel wall/endothelium/oxidative metabolism)

AMY G. TSAI*†, BARBARA FRIESENECKER*‡, MICHELLE C. MAZZONI*§, HEINZ KERGER*¶, DONALD G. BUERK‖, PAUL C. JOHNSON*, AND MARCOS INTAGLIETTA*

*Department of Bioengineering, University of California, San Diego, La Jolla, CA 92093-0412; and ‖Departments of Physiology and Bioengineering, and the Institute for Environmental Medicine, University of Pennsylvania, Philadelphia, PA 19104-6086

Communicated by Yuan-Cheng B. Fung, University of California, La Jolla, CA, March 27, 1998 (received for review May 14, 1997)

ABSTRACT **One of the most important functions of the blood circulation is O_2 delivery to the tissue. This process occurs primarily in microvessels that also regulate blood flow and are the site of many metabolic processes that require O_2. We measured the intraluminal and perivascular pO_2 in rat mesenteric arterioles *in vivo* by using noninvasive phosphorescence quenching microscopy. From these measurements, we calculated the rate at which O_2 diffuses out of microvessels from the blood. The rate of O_2 efflux and the O_2 gradients found in the immediate vicinity of arterioles indicate the presence of a large O_2 sink at the interface between blood and tissue, a region that includes smooth muscle and endothelium. Mass balance analyses show that the loss of O_2 from the arterioles in this vascular bed primarily is caused by O_2 consumption in the microvascular wall. The high metabolic rate of the vessel wall relative to parenchymal tissue in the rat mesentery suggests that in addition to serving as a conduit for the delivery of O_2 the microvasculature has other functions that require a significant amount of O_2.**

Blood entering capillaries is only 50% saturated (1), thus one-half of the O_2 gathered by the lung exits the circulation before arrival in the capillaries. This rate of O_2 loss from the arteriolar network has been found and documented in different species and tissues at rest (2–7). It was noted in one study that this loss is an order of magnitude greater than expected from simple diffusion (8). Possible sinks for the O_2 exiting before the capillaries include O_2 shunting from arterioles to parallel venules (9), periarteriolar tissue consumption (10), and arteriolar-capillary O_2 diffusional shunting (11). The contribution of arterio-venous shunting appears to be negligible during normal conditions (9), and although arteriocapillary diffusional shunting has been demonstrated (11), the conditions under which it might occur, i.e., an arteriole crossing a capillary network, are not common in the mesentery. It therefore is important to examine in detail the loss of O_2 from arterioles to surrounding tissue. The outward flux of O_2 from blood is governed by the law of diffusion and defined by O_2 gradients between blood and the surrounding tissue. O_2 delivery to the tissue surrounding the microvessels has not been extensively studied because of the lack of methods that can measure pO_2 in both blood and tissue. Recently, an optical method has been developed that makes such a study feasible (12).

The objective of our study was to use noninvasive phosphorescence quenching microscopy to determine the radial pO_2 profiles *in vivo* for the periarteriolar tissue of the rat mesentery. With this method it was possible to determine the contribution of microvascular wall metabolism to the precapillary O_2 exit. Intravascular and extravascular measurements were carried out by using the same pO_2 measuring technique, and validation of tissue fluxes was obtained by O_2 mass balance between O_2 entering and exiting vascular segments, and the O_2 diffusional fluxes were determined by the measured O_2 gradients.

MATERIALS AND METHODS

Phosphorescence Quenching Microscopy. Pd-phosphorescence quenching microscopy, based on the relationship between the decay rate of excited Palladium-mesotetra-(4-carboxyphenyl)porphyrin (Porphyrin Products, Logan, UT) bound to albumin and the pO_2 according to the Stern-Volmer equation, was used to measure pO_2 in the microcirculation (13). The method was used previously in microcirculatory studies to determine blood pO_2 levels in different tissue under different conditions (14–18). In our system, a xenon strobe (EG & G, Salem, MA; decay constant of 10 μsec, frequency of 30 Hz; peak wave length of 420 nm) excites the phosphorescence by epi-illumination of a tissue area for 3 sec. Phosphorescence emission from the target tissue area passes through an adjustable rectangular optical slit and light filter (630-nm cutoff) and is captured by a photomultiplier (EMI, 9855B; Knott Elecktronick, Munich, Germany). A digital oscilloscope (Tektronix, 2434) averages 90 photomultiplier decay signals, and the resulting smoothed curve is stored to a computer. Decay curves are analyzed off-line, by using a standard single exponential least-squares numerical fitting technique, and the resultant time constants are applied to the Stern-Volmer equation to calculate pO_2, where k_Q, the quenching constant and τ_0, the phosphorescence lifetime in the absence of O_2 measured at pH = 7.4 and T = 37°C are 325 $mmHg^{-1}\,sec^{-1}$ and 600 μs, respectively. The phosphorescence decay caused by quenching at a specific pO_2 yields a single decay constant (12), and *in vitro* calibration has been demonstrated to be valid for *in vivo* measurements.

As a consequence of the two-dimensional, single-layer planar characteristic of the vasculature in the exteriorized mesentery preparation, our phosphorescence exponential decay signal is not contaminated by signals from vessels above and below the focus plane and usually is fitted with a high level of correlation ($r > 0.92$) by a single exponential. Modeling of the decay curves obtained from our measurements as multiple exponentials does not alter the results obtained with a single exponential fit. Our measurements, based on minimal and

The publication costs of this article were defrayed in part by page charge payment. This article must therefore be hereby marked "*advertisement*" in accordance with 18 U.S.C. §1734 solely to indicate this fact.

†To whom reprint requests should be addressed. e-mail: agtsai@ucsd.edu.
‡Present address: Department of Anesthesia and Intensive Care Medicine, The Leopold-Franzens-University of Innsbruck, Innsbruck, Austria.
§Present address: Alliance Pharmaceutical Corp., San Diego, CA 92121.
¶Present address: Institute for Anesthesiology and Operative Intensive Care, Mannheim, Heidelberg University, Mannheim, Germany.

uniform light exposure, do not show evidence of changes in phosphorescence intensity within the tissue near the vessel wall. Furthermore, we found no change in the measured pO_2 distribution when using windows slits of widths varying from 7.5 to 20 μm for characterizing the gradient when the center line of the window was assumed to be the location of the measurement, indicating that the window provides a consistent average of the decay curves within the window.

Interstitial pO_2 Measurement. The albumin-bound probe passes into the interstitium according to the exchange of albumin from blood to tissue (19). The resulting accumulation of albumin-bound dye within the tissue, which may contain up to 10% of the total albumin in the organism, allows measurement of tissue and intravascular pO_2 at high resolution with the same technique. The reflection coefficient of albumin in different vascular networks varies, changing the equilibration time between intravascular and extravascular dye/albumin. Because measurement of pO_2 is possible anywhere Palladium-porphyrin albumin-bound complex is located given an adequate signal-to-noise ratio (15–17), in our model tissue pO_2 measurements could be made within 20 min after injection. Interstitial pO_2 profiles were determined by measuring pO_2 in the tissue at specific distances from the vessel lumen.

Phosphorescence generated by the light excitation of the porphyrin probe consumes O_2. This photoactivation could be a factor affecting tissue O_2 measurements made in a slow-moving or stationary fluid. To determine the extent of this photoactivation on our interstitial measurements, we performed *in vitro* measurements in sealed tubes. We estimated O_2 consumption by the technique in sealed 75-mm long hematocrit tubes filled with Pd-meso-tetra(4-carboxyphenyl-)porphyrin bound to albumin solution (0.1 mg/ml) saturated to pO_2 of 37 mmHg with the same system used for animal experiments. The concentration of probe used is approximately that which would be found in interstitial fluid. Albumin concentration in tissue at steady state is approximately one-third lower than in blood, therefore the probe concentration of 0.26 mg/ml plasma within the blood (= 10 mg/ml probe $\times$ 0.1 ml probe/100 g animal $\times$ 100 g animal/7.0 ml blood $\times$ 1 ml blood/0.55 ml plasma) corresponds to an interstitial fluid probe level of 0.09 mg/ml. The initial pO_2 within the tube was measured at three locations 1.5 mm apart with a 3-sec, 30 flashes/sec pulsed light. The center of the tube was masked and exposed to 45 min of pulsed illumination at a rate of 30 flashes/sec, in such a fashion that 0.5 mm of tube length was exposed to flash illumination. Immediately after the pulsed exposure, the tube content was mixed by a nylon bar sealed in the tube, which was made to move by gravity along the length of the tube for 5 sec in each direction during a 5-min period. PO_2 measured in the tube at the three locations decreased from 37 to 31 mmHg. Therefore 81,000 light flashes lowered pO_2 within the exposed tube segment by (6 mmHg $\times$ 75 mm/0.5 mm $\times$ 8.1×10^4) = 0.01 mmHg/flash. The decrease in O_2 at the excitation spot was initially a factor of 2 higher than the rate determined for the entire flashing period. O_2 initially is consumed solely at the excitation spot, establishing a concentration gradient whereby consumption is lowered by diffusion of O_2 from surrounding areas into the excitation spot.

We used 90 flashes (3 sec) for each measurement. We estimate that the free fluid in the mesentery in which albumin-bound probe is present is at most 20% of the total tissue volume; the rest of the tissue is not occupied by the probe and constitutes a reservoir of O_2. Therefore the maximal reduction in pO_2 during each determination, assuming the highest rate found for O_2 consumption by the flash, is about 0.02 mmHg/flash $\times$ 90 flashes $\times$ 0.2 = 0.4 mmHg.

We also examined the accuracy of the tissue pO_2 measurements with the phosphorescence method *in vivo* by simultaneous continuous measurements with approximately 5-μm diameter recessed tip gold cathode microelectrodes (20). Measurements were made in avascular tissue areas of the hamster skin fold preparation (15–17). In these studies, the tissue was isolated from extraneous sources of O_2 by superfusing with a Krebs Henseleit solution (1.3×10^{-1} M NaCl, 1.2×10^{-3} M Mg SO_4, 2.0×10^{-3} M $CaCl_2$, 4.7×10^{-3} M KCl, 2.2×10^{-2} M $NaHCO_3$) bubbled with 100% N_2. A maximum divergence of 2% was found between the methods over the tissue pO_2 range of 5–40 mmHg. Extended flashing over a period of up to 1 min did not produce a detectable change in the microelectrode measurement. The congruence between microelectrode and phosphorescence quenching microscopy measurements demonstrates that excitation of the porphyrin probe in the tissue is minimal and does not affect tissue pO_2 in our model. It should be noted that those investigators (15–17) using the same technique reported that capillary pO_2 in the hamster skin fold preparation was 29 mmHg, tissue pO_2 was 23 mmHg, and the gradient at the capillary wall was 4 mmHg (21). This finding is incompatible with the assumption that the pO_2 decrease on the order of 20 mmHg found near arterioles is caused by O_2 consumption by the dye in the tissue, because capillaries have 100-fold lower O_2 delivery capacity than the arterioles in this study, which would result in a near-zero pericapillary tissue pO_2 measurement.

Mesentery Preparation. The mesentery of male Wistar rats (250–350 g) was exteriorized, and the upper and lower surfaces of the tissue were sandwiched between two essentially gas-impermeable and transparent barriers, allowing O_2 to exit from the vasculature only in the plane of the tissue as shown diagrammatically in Fig. 1. After anesthetizing the animal (Nembutal, 40 mg/kg i.m. into left hind limb), the right femoral vein and artery are cannulated for: (*i*) injection of Pd-phosphorescence probe and supplemental anesthesia (5–10 mg/kg), and (*ii*) monitoring blood pressure. The animal is placed on a microscope stage with a circulating water heater (37°C). The mesentery is exteriorized through an epigastric incision, partially extracted, and kept moist with dripped buffered Krebs Henseleit solution, pH corrected by bubbling a gas mixture of 5% CO_2 and 95% N_2. It is viewed by draping it over a thin circular glass platform. Before the experiment the

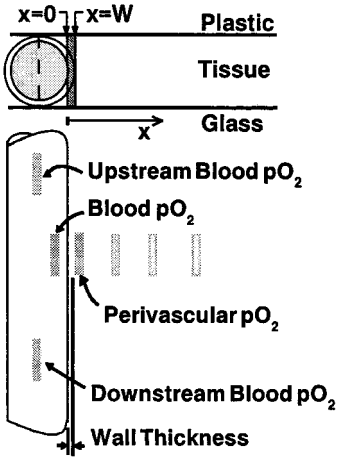

FIG. 1. (*Upper*) The geometry of the exteriorized mesentery preparation. Mesentery is sandwiched between O_2 impermeable upper and lower barrier of plastic and glass. Circle represents blood vessel with vessel wall. O_2 diffuses in the planar, x, direction, $x = 0$ is the blood side of the blood/tissue interface. W is the thickness of the vessel wall. (*Lower*) The positions of the optical window (shaded rectangles) are shown schematically. Upstream and downstream pO_2 along with vessel diameter, blood velocity with a given separation distance is used to calculate the convective O_2 losses. O_2 mass balance is studied by comparing O_2 loss along and diffusional loss out of the vessel. pO_2 levels detected in blood and at increments in tissue, illustrated by the staggered window in x-direction are used to construct pO_2 profiles. Window size was a 5 μm $\times$ 20 μm rectangle.

tissue is covered with a thin strip of transparent plastic film (Saran, Dow Corning) to prevent gas exchange [diffusion coefficient of 6.2×10^{-13} cm^3 O_2/(cm × mmHg × sec)] and desiccation. The heated drip without the gas is continued onto the plastic to maintain tissue at 37°C during the study. A temperature probe (Physitemp, Clifton, NJ) was placed on the plastic and positioned above the mesenteric window under study to monitor tissue temperature during the experiment.

Experimental Protocol. The animal was positioned on an inverted microscope (IMT-2, Olympus, New Hyde Park, NY) equipped with a 40× objective (WPlan FL40x, 0.7 water). Measurements began 20 min after injection of phosphorescence probe (10 mg/ml, 0.1 ml/100 g). Transillumination (halogen lamp, 12 V, 100 W) was used to measure vessel diameter (22) and blood flow velocity (23), followed by intravascular and perivascular pO_2 determinations using phosphorescence quenching microscopy. Transillumination measurements were made with a maximum of 2–3 V power to the lamp to reduce possible light toxicity and photoactivation of the phosphorescence probe. All pO_2 measurements were performed after extraneous light from the transillumination lamp and the room were eliminated. Each intravascular pO_2 measurement was repeated after perivascular pO_2 determinations to assure constant delivery conditions were maintained. Vessels whose intravascular pO_2 readings differed by more than 5 mmHg were not included in the study. Measurements were obtained in vessels with sharp focus and not in close proximity to other vessels (>250 μm separation). The optical measuring windows (5 μm × 20 μm) were placed as shown in Fig. 1 relative to the vasculature under study. Extravascular pO_2 profiles were obtained by progressively displacing the optical measuring window away from the blood/tissue interface. All measurements were performed within a 30-min period. The resolution of the optical window does not allow for pO_2 measurements within the vascular wall.

Vessel Wall Gradient. In this model, an O_2 gradient between blood and perivascular tissue greater than that dictated by simple diffusion is indicative of O_2 consumption by the vessel wall when the calculated diffusion flux shows mass balance with the decrease of O_2 content in the flowing blood. Thus the vessel wall gradient, the difference between intra- and perivascular pO_2, was used to determine the rate of vessel wall oxidative metabolism and later used in determining the mass balance in vessel segments. The perivascular pO_2 profile was used to calculate tissue oxidative metabolism. The pO_2 measured in tissue adjacent to the O_2 source (about 4 μm from the blood-tissue interface) could, in principle, be contaminated by the higher intensity phosphorescence decay signal from blood. The net effect of this contamination, if it exists, would result in a higher perivascular pO_2 reading and thus underestimate the measured vessel wall gradient.

Theoretical Simulation and Analysis. Our system consisting of a thin tissue whose thickness is much less than the distance between adjacent vessels, can be modeled in terms of diffusion from a linear source (the blood vessels) with thickness equal to that of the tissue (assumed to be identical to the separation between the impermeable barriers). This process is described by Fick's law of diffusion for O_2 into a semi-infinite region extending away from the source in the x direction, where the consumption rate is g and the diffusivity is D. The governing equation at steady state is:

$$\alpha D\ (d^2p/dx^2) - g = 0, \qquad \textbf{[1]}$$

where p = oxygen tension and α = solubility constant for O_2. We assume that there is no O_2 gradient perpendicular to the tissue plane and that the mesentery is a homogenous tissue with a constant rate of O_2 consumption.

Tissue and Vessel Wall Metabolic Rate. With boundary conditions of a constant O_2 source p_W at the vessel wall/tissue interface $x = W$ and a no flux of O_2 at a penetration distance δ from vessel wall/tissue interface, the solution of Eq. **1** is:

$$p(x) = K_0\,x^2 + K_1\,x + K_2. \qquad \textbf{[2]}$$

The coefficients are $K_O = g/(2D\alpha)$, $K_1 = -(g\delta)/(D\alpha)$, and $K_2 = p_W - [(gW)/(D\alpha)][(W/2)-\delta]$; W, is the location of the vessel/tissue interface. Curve fitting of the perivascular pO_2 profiles to the second-order polynomial solution was used to determine the tissue consumption rate from the coefficient K_o. The distance of O_2 penetration from the vessel wall/tissue interface, δ, is determined from K_1.

A finite difference numerical approximation of Eq. **1** is used to calculate the steady-state profile for the perivascular tissue, consisting of two metabolically active regions representing the vascular wall and the tissue proper. By using the consumption rate of tissue obtained with curve fitting and the distance of O_2 penetration, the rate of vessel wall metabolism is iterated until the measured intra- and perivascular difference is attained. The boundary and regional conditions are: (*i*) At blood side of blood/tissue interface, $x = 0$, O_2 tension is equal to intravascular pO_2, $p = p_i$; (*ii*) At interface between vessel wall p_w and tissue p_T, $x = W$, O_2 flux is continuous $D\alpha\ (dp_w/dx) = D\alpha\ (dp_T/dx)$; (*iii*) At penetration distance, $x = \delta$, O_2 level is constant, $dp/dx = 0$; (*iv*) g_W, O_2 consumption rate in region comprising the vessel wall ($0 < x \leq W$); and (*v*) g_T, O_2 consumption rate in region beyond the vessel wall ($x > W$) to the penetration depth ($x = \delta$).

Mass Conservation Analysis of O_2 Transport. The law of mass conservation stipulates that the amount of O_2 lost from a vascular segment must be equal to the diffusional O_2 flux, determined by the perivascular pO_2 gradient. We studied longitudinal and radial O_2 losses from nonbranching vessel segments to determine the extent of O_2 loss in our animal model. The equation for the rate of longitudinal O_2 loss along the length of a microvessel is:

Change in longitudinal O_2 flux

$$= (\mathrm{Q}[\mathrm{O_2}])_{\mathrm{upstream}} - (\mathrm{Q}[\mathrm{O_2}])_{\mathrm{downstream}}, \qquad \textbf{[3]}$$

where $Q = v\pi r^2$ and $[O_2] = C_b\ [fHCT]\ SO_2$. The parameters are: Q, blood flow; v, blood flow velocity, corrected for velocity profile shape (24); r, vessel radius; $[O_2]$, O_2 content; C_b, O_2 binding capacity of blood; $[fHCT]$, ratio of microvascular to systemic hematocrit, a function of vessel diameter (25) (physically dissolved O_2 is neglected because of low solubility of O_2 in plasma); SO_2, hemoglobin O_2 saturation, intravascular pO_2 measurements are converted to SO_2 (26).

Longitudinal O_2 exit must be matched by the rate of O_2 exit by diffusion and O_2 consumption by the vessel wall. The area through which O_2 diffuses out of the blood vessel into the tissue is assumed to be the plane perpendicular to the impermeable barriers. The remaining portion of the blood vessel, V_W, in contact with the impermeable barriers is assumed to consume O_2 at the experimentally determined rate g_w. However this portion of the vessel wall does not contribute to the diffusive flux into the tissue. This rate of O_2 exit by diffusion and O_2 consumption by the vessel wall is expressed as

Diffusive O_2 flux and O_2 wall consumption

$$= DA\,\alpha[p_i - p_o]/dx + V_w g_w; \qquad \textbf{[4]}$$

where D, diffusivity (1.70×10^{-5} cm^2/sec) (27); A, surface area; α, O_2 solubility constant (2.14×10^{-5} ml O_2/cm^3 mmHg) (27); p_i, intravascular pO_2; p_o, perivascular pO_2; dx, vessel wall thickness, approximated as 10% of vessel diameter (2.3 μm); V_W, volume of vessel wall; g_w, O_2 consumption rate of vessel wall determined by the theoretical analysis of measured tissue pO_2 profiles.

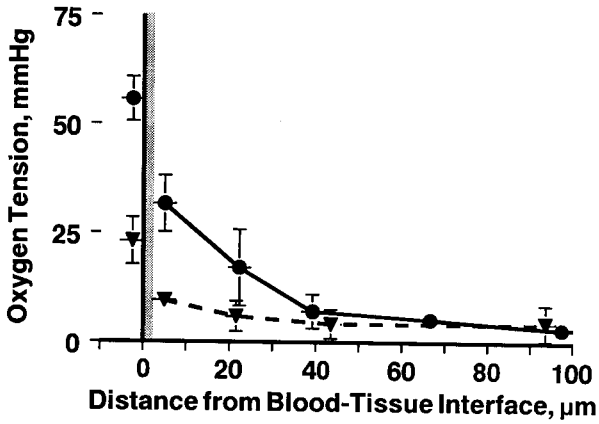

FIG. 2. Large drop in pO_2 across the blood/tissue interface. PO_2 profiles from blood into tissue for high (●) and low (▲) intravascular pO_2. Results were grouped according to intravascular pO_2 levels. Intravascular pO_2 measurements were made flush to the intraluminal vessel wall with the center of the window slit 2.5 μm from the vessel wall. Perivascular pO_2 begins with the window flush with the abluminal vessel wall. The solid horizontal bars at each data point represent the width of the rectangular slit. The vascular wall is depicted as the shaded area. Individual measurements from different profiles are grouped as function of distance from intraluminal wall (mean ± SD).

Curve fitting to the data was performed by first transforming the data to allow for linear least-squares regression. Gauss-Jordan method for matrix inversion then was used to determine the coefficients from the transformed data (Table Curve 2-D, Jandel, San Rafael, CA). Results are presented mean ± standard error unless otherwise stated.

RESULTS

PO_2 profiles were obtained in 12 animals from 31 arterioles with sharp focus and not in close proximity to other vessels (>250-μm separation). Results were grouped according to intravascular pO_2 levels ($p_i > 50$; $40 < p_i \leq 50$; $30 < p_i \leq 40$; and, $20 < p_i \leq 30$ mmHg). Profiles for two groups are shown in Fig. 2 to demonstrate the pronounced fall between intravascular ($x = 0$) and perivascular ($x = 5$ μm) pO_2, a distance spanning the vessel wall, which includes endothelium and smooth muscle. The finding of a steep fall in pO_2 near the vessel wall was common to all groups. Fig. 3 shows a more closely sampled pO_2 profile, which exhibits the same characteristics as those more sparsely sampled profiles used in the analysis.

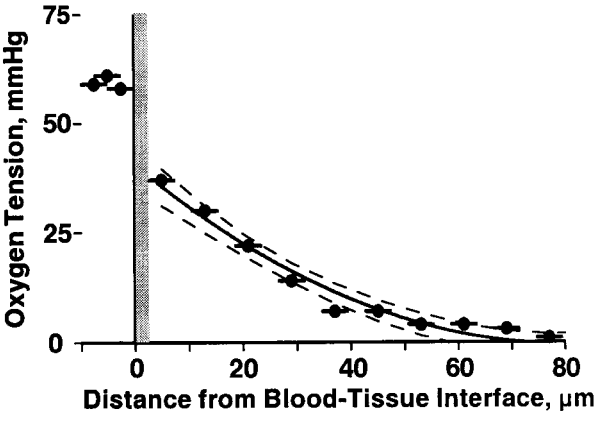

FIG. 3. Example of pO_2 profile found in the rat mesentery. Closely sampled pO_2 measurements allow for a detailed view of tissue pO_2 profile. Solid line is the curve fitting of the pO_2 profile within the tissue, dotted lines are the 95% confidence intervals of the data. Intravascular pO_2 averaged 59.3 ± 1.5 mmHg (horizontal bar), shown left of the blood tissue-interface. The wall was taken to be 2.5 μm thick, and each data point represents the pO_2 within the sampling window whose width is represented by the horizontal bars.

The theoretical profile for diffusion from a constant source into a consuming medium was constructed to determine whether measured pO_2 profiles corresponded to a region with a single metabolic rate, implying that vessel wall O_2 consumption is equal to that in the tissue proper, or whether the vessel wall and tissue have different metabolic rates (Eq. **2**). The measured tissue pO_2 profiles were fitted to the theoretical solution for the tissue region beyond 2.5 μm of the blood/tissue interface to determine the tissue O_2 consumption rate and penetration. Average g_T and δ for all groups were $2.4 \times 10^{-4} \pm 0.5$ ml O_2/(cm^3 tissue sec) and 93.6 ± 11.1 μm, respectively. Least-squares regression correlation coefficients of the curve fit to the profiles ranged from $r = 0.87$ to 0.99, being all statistically significant $P < 0.01$. Fig. 4 shows the mean pO_2 profile from the $pO_2 > 50$ mmHg group and the curve fit used to determine the tissue O_2 consumption rate.

The two-compartment model was used to determine the vessel wall O_2 consumption rate relative to the tissue. We found the average vessel wall metabolic rate needed to achieve the intravascular pO_2 levels given the tissue pO_2 profiles was 277.8 ± 45.0 (range 141–323) times that of the tissue metabolic rate or 3.9 ml O_2/(cm^3 tissue min).

If the O_2 consumption of the vessel wall is as great as the calculation above suggests there should be a corresponding loss of O_2 longitudinally. Therefore we measured the rate of O_2 exit both longitudinally and radially in 12 vessel segments of five animals. Longitudinal saturation drop was 2.4 ± 0.3%/100 μm in vessels with average diameter of 23.2 ± 2.9 μm and blood flow velocity of 1.5 ± 0.3 mm/sec. Intravascular pO_2 was 43.3 ± 3.7 mmHg and the intraperivascular difference was 18.1 ± 1.7 mmHg.

Loss of O_2 along each individual vessel segment (Eq. **3**) was found to be within 3.3 ± 19.6% of their diffusional losses (Eq. **4**), confirming that the rate of O_2 exit is caused by the extremely large O_2 gradient in the tissue compartment that includes the vessel wall. The average convective loss of $2.4 \pm 0.5 \times 10^{-5}$ ml O_2/cm^2 sec and diffusive loss of $2.2 \pm 0.2 \times 10^{-5}$ ml O_2/cm^2 sec in all of the vessels studied agreed within 8.6%. Calculation of O_2 loss from averaged parameters does not yield

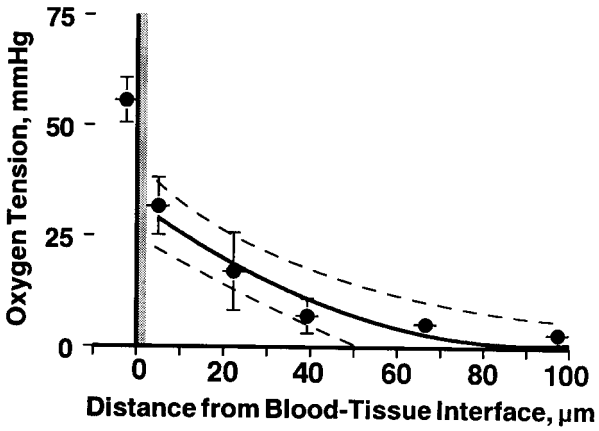

FIG. 4. Graph shows curve fitting to the tissue profile with tissue having one consumption rate. An average g_T of $2.4 \times 10^{-4} \pm 0.5$ ml O_2/(cm^3 tissue sec) and δ of 93.6 ± 11.1 μm were determined from the coefficients. Least-squares regression correlation coefficient of the curve fit to the perivascular portion of the pO_2 profiles is $r = 0.98$, and the dotted line represents the 95% confidence intervals. When the two-compartment model is used to fit the tissue pO_2 profile with the intravascular pO_2 of 55.6 mmHg, the vessel wall consumption rate was found to be 141 times the tissue rate. Data is grouped axially and presented as mean ± SD ($n = 6$ profiles).

mass balance because the parameters that determine O_2 fluxes are not related in an additive form.

DISCUSSION

This study shows that there is a substantial O_2 loss from the blood as it passes through the arteriolar network in the rat mesentery. This was first reported by Duling and Berne (1) using recessed microelectrodes in the hamster cheek pouch and subsequently in other laboratories (2–7) using microelectrode and spectrophotometric measurement techniques.

In addition to the large O_2 loss, we found a large pO_2 gradient across a tissue region that includes the arteriolar vessel wall. The presence of this gradient can account for the large rate of O_2 loss from microvessels because, in accordance with the law of mass balance, our results require that the large rate of O_2 exit from arterioles be driven by a large O_2 gradient. The steep O_2 gradient across the wall could be caused by a large amount of O_2 consumption or an increased diffusional resistance within the vessel wall (lower diffusion constant and/or permeability). However, in the latter case the resulting steep gradient would lead to significantly lower O_2 exit, and therefore a large difference between longitudinal O_2 loss and tissue O_2 flux and a large disparity in mass balance.

The low levels of pO_2 in the tissue (and therefore large gradients) could be caused by O_2 consumption by the technique because the fluid containing the probe in the tissue is virtually stationary during the period of measurement. Intravascular measurements would not be affected by O_2 consumption because the blood flow would replace the consumed O_2. Simultaneous measurements of tissue pO_2 levels using our phosphorescence decay system and recessed microelectrodes found no statistical change in pO_2 during our 3-sec measurement period or during prolonged flashing. Moreover when using the phosphorescence technique to measure tissue pO_2 in the hamster skin fold chamber we found values between 23 and 25 mmHg (7, 15–17), similar to the value of 26 mmHg reported by Endrich *et al.* (28), who used surface platinum multiwire electrodes in the same tissue. Our values obtained using the phosphorescence technique are higher than those reported with microelectrode measurements in the hamster cremaster muscle, which ranged from 11 to 17 mmHg (29, 30). Therefore our tissue pO_2 measurements are within the range of previous measurements made by other investigators using different techniques and are not unduly lowered by photoactivation of the phosphorescence probe.

Our *in vitro* measurements of the amount of O_2 consumption per flash described in *Materials and Methods* also corroborated the electrode findings that O_2 quenching by photoactivation of the probe is not a factor affecting our measurements. The equivalent lowering of tissue pO_2 was found to be about 0.4 mmHg. This number is indicative of the maximum possible error in the measurement; however, the actual error is much smaller because as O_2 is consumed it also is replenished by diffusion from the arteriole. Tissue O_2 depletion by flash illumination in the area of measurement (about 140 μm in diameter, 50 μm thick) is calculated to be 1.4×10^{-12} ml O_2/sec, whereas the arterioles supply O_2 at a rate of 4.1×10^{-9} ml O_2/sec, or a rate that is about 3,000 times greater than that at which O_2 is consumed by the probe during the measurement, indicating that pO_2 measurements are not affected by probe O_2 consumption near the vessel wall.

The spatial resolution of our technique is not sufficient to measure the pO_2 profile within the vessel wall; however, we can accurately measure the pO_2 difference across the vessel wall. To measure pO_2 as close as possible to the blood-tissue interface, the optical windows were as narrow as possible, compatible with the need for adequate signals. The tissue pO_2 profile also was determined with a window that was 10 μm by 20 μm, double the width used in this study, and there was no difference in the pO_2 measurements even in regions of steep gradients, indicating that in these experiments pO_2 is averaged within the window.

In our mass balance calculations, we approximated vessel wall thickness to be 10% of the average vessel diameter. We found that vessel wall thickness of the vessels studied ranged from 1.3 to 7.5 μm, the magnitude greatly depending on the position of the nucleus of endothelial cells and smooth muscle cells. Wall thickness tends not to be uniform in these vessels, and we used an average wall thickness based on the lumen size. Varying the vessel wall thickness from 2 to 3 μm in our mass balance calculations shifted the balance between O_2 loss along each vessel segment and the diffusional flux to deviate by -5.6% and 17.0%, respectively.

Our measurements of the pO_2 gradient in the mesentery itself provides an estimate of O_2 consumption rate of mesenteric tissue of $2.4 \pm 0.5 \times 10^{-4}$ ml O_2/cm^3 tissue sec, which is about four times higher than the value for loose connective tissue of 5.6×10^{-5} ml O_2/cm^3 tissue sec determined from the renal capsule of the goat (31), a comparison between the same tissue type but from different size animals. O_2 consumption relative to the body size is much higher in smaller than in the larger mammals. By using the empirical relationship of mammals size and O_2 consumption, assuming that connective tissue also can be similarly scaled, we estimate that the O_2 consumption rate of the rat to be on the order of 3–4 times higher than the goat (32), and therefore similar to the one found in this study.

Investigations in other tissues and models that used different measurement techniques also found evidence of a high rate of vessel wall metabolism. When endothelium is removed from the dog hind limb O_2 consumption decreases by 34% (33). Measurements in larger arterial vessels using microelectrodes show that the ratio between the O_2 consumption rate and the diffusivity increases nearly 10-fold as the electrode is advanced from the abluminal side toward the blood/vessel interface (34). Therefore given a constant diffusivity the rate of O_2 consumption increases significantly near the blood/vessel interface. However, the O_2 consumption rate suggested by that study was significantly lower than the one we measured, a discrepancy that may be, in part, because of the resolution limitation of 10–15 μm microelectrode tips. Investigations of O_2 consumption by endothelial cells cultured from vascular tissue found a metabolic rate "as much as 5,000-fold" over the rate in organized tissues (35).

The endothelial lining of blood vessels has, until recently, been regarded as simply a barrier between the blood and the parenchyma, greatly restricting passage of macromolecules while allowing rapid exchange of gases and crystalloids. Mitochondria density is not particularly pronounced within endothelium (36) and cannot solely account for the high respiratory rate of the vessel wall suggested by our findings. However, endothelial cells are the site of chemical synthesis and metabolic processes that require O_2 (renin, prostaglandins, collagen, conversion of angiotensin I to II, degradation of bradykinin and prostaglandins, and the clearance of lipids and lipoprotein) (37). The endothelium is a principal mediator in many homeostatic (38) and disease processes (39, 40) and has been considered a widely influential "organ" (41). Moreover, endothelial cells have an active actin/myosin-based contractile system that also may consume O_2 (42, 43). In the blood/tissue interface, endothelium overlays and interacts with smooth muscle throughout the vasculature with the exception of the capillaries, giving origin to the regulatory mechanism that modulates the vessel diameter and controls tissue perfusion. The metabolic cost of this array of endothelial function has not been addressed previously. It is worth noting that because of its location, the endothelium has the highest O_2 availability of all tissues.

Previous studies on microvascular O_2 distribution relied on a spectrophotometric method for intravascular O_2 determination and electrode measurements to characterize tissue pO_2 gradients. Those studies were carried out either longitudinally or radially, but only rarely in both directions with the same technique. Lack of direct evidence for steep gradients at the vessel wall led to the concept that the O_2 diffusion constant for the arteriolar wall may be an order of magnitude larger than that of water to account for the large rate of O_2 loss (8).

Microelectrode studies by Duling *et al.* (2) in pial vessels of the cat revealed both a longitudinal gradient along the vessel and transmural gradient across the vessel wall. They found a difference between blood pO_2 and vessel surface pO_2, which ranged from 27 mmHg in the largest (234 μm diameter) to 6 mmHg in the smallest (22 μm diameter) arterioles. O_2 consumption by the wall was estimated to be 2.8×10^{-2} ml O_2/sec g tissue, which is similar to our finding. Yaegashi *et al.* (44) in their study of pO_2 distribution in mesenteric microcirculation, which used O_2-sensitive fluorescence-coated 3-μm silica gel beads embedded in a silicone rubber membrane 5 μm thick suspended an average 38 μm above the mesenteric surface, found a longitudinal pO_2 gradient three times smaller than the value reported by ourselves and others. Their study did not find the wall pO_2 gradient seen in our study. Because of the separation of the O_2-sensitive membrane and the tissue surface, this method may have limited resolution. From their measurements, they estimated O_2 consumption rate in the rat mesentery to be 8.2×10^{-6} ml O_2/cm^3 tissue sec, which is 30 times lower than our finding.

The metabolic rate of endothelium may vary among organs and vessels within the same organs as they all are subjected to different local conditions and influences. Our finding of a high metabolic rate in the wall of mesenteric arterioles may help to explain in part the large O_2 loss observed in other arteriolar networks in other tissues but this requires further study.

In summary, this report documents the existence of steep O_2 gradients at the wall of arterioles in the rat mesentery. The steepness of the O_2 gradient is compatible with the hypothesis that the arteriolar vessel wall is a region of high O_2 consumption. This finding in the rat mesentery suggests that O_2 delivery to parenchymal tissue is, in part, determined by the vessel wall metabolism in the microcirculation.

This study was supported by U. S. Public Health Service–National Heart, Lung and Blood Institute Grant HL-48108.

1. Duling, B. R. & Berne, R. M. (1970) *Circ. Res.* **27,** 669–678.
2. Duling, B. R., Kuschinsky, W. & Wahl, M. (1979) *Pflügers Arch.* **383,** 29–34.
3. Pittman, R. N. & Duling, B. R. (1977) *Microvasc. Res.* **13,** 211–224.
4. Ivanov, K. P., Derii, A. N., Samoilov, M. O. & Semenov, D. G. (1982) *Pflügers Arch.* **393,** 118–120.
5. Swain, D. P. & Pittman, R. N. (1989) *Am. J. Physiol.* **256,** H247–H255.
6. Buerk, D. G., Shonat, R. D., Riva, C. E. & Cranstoun, S. D. (1993) *Microvasc. Res.* **45,** 134–148.
7. Torres Filho, I. P., Kerger, H. & Intaglietta, M. (1996) *Microvasc. Res.* **51,** 202–212.
8. Popel, A. S., Pittman, R. N. & Ellsworth, M. L. (1988) *Am. J. Physiol.* **256,** H921–H924.
9. Sharan, M. & Popel, A. S. (1988) *Math. Biosci.* **91,** 17–34.
10. Kuo, L. & Pittman, R. N. (1990) *Am. J. Physiol.* **259,** 1694–1702.
11. Ellsworth, M. L. & Pittman, R. N. (1990) *Am. J. Physiol.* **258,** H1240–H1243.
12. Vanderkooi, J. M., Maniara, G., Green, T. J. & Wilson, D. F. (1987) *J. Biol. Chem.* **262,** 5476–5482.
13. Torres Filho, I. P. & Intaglietta, M. (1993) *Am. J. Physiol.* **265,** H1434–H1438.
14. Helmlinger, G., Yuan, F., Dellian, M. & Jain, R. K. (1997) *Nat. Med.* **3,** 177–182.
15. Kerger, H., Saltzman, D. J., Menger, M. D., Messmer, K. & Intaglietta, M. (1996) *Am. J. Physiol.* **270,** H827–H836.
16. Kerger, H., Torres Filho, I. P., Rivas, M., Winslow, R. M. & Intaglietta, M. (1995) *Am. J. Physiol.* **267,** H802–H810.
17. Kerger, H., Saltzman, D. J., Gonzales, A., Tsai, A. G., van Ackern, K., Winslow, R. M. & Intaglietta, M. (1997) *Anesthesiology* **86,** 372–386.
18. Shonat, R. D., Richmond, K. N. & Johnson, P. C. (1995) *Rev. Sci. Instrum.* **66,** 5075–5084.
19. Parker, J. C., Perry, M. A. & Taylor, A. E. (1984) in *Edema*, eds. Staub, N. C. & Taylor, A. E. (Raven, New York), pp. 7–27.
20. Whalen, W. J., Riley, J. & Nair, P. (1965) *J. Appl. Physiol.* **23,** 789–794.
21. Intaglietta, M., Johnson, P. C. & Winslow, R. M. (1996) *Cardiovasc. Res.* **32,** 632–643.
22. Intaglietta, M. & Tompkins, W. R. (1973) *Microvasc. Res.* **5,** 309–313.
23. Intaglietta, M., Silverman, N. R. & Tompkins, W. R. (1975) *Microvasc. Res.* **10,** 165–179.
24. Pittman, R. N. & Ellsworth, M. L. (1986) *Microvasc. Res.* **32,** 371–388.
25. Kanzow, G., Pries, A. R. & Gaehtgens P. (1982) *Int. J. Microcirc. Clin. Exp.* **1,** 67–79.
26. Ulrich, P., Hilpert, P. & Bartels, H. (1963) *Arch. Gesamte Physiol.* **277,** 150–165.
27. Middleman, S. (1972) in *Transport Phenomena in the Cardiovascular System.* (Wiley Interscience, New York), pp. 53 and 131.
28. Endrich, B., Goetz, A. & Messmer, K. (1982) *Int. J. Microcirc. Clin. Exp.* **1,** 81–99.
29. Gorczynski, R. J. & Duling, B. R. (1978) *Am. J. Physiol.* **235,** H505–H515.
30. Klitzman, B., Popel, A. S. & Duling, B. R. (1982) *Microvasc. Res.* **25,** 108–131.
31. Lentner, C. (1986) in *Geigy Scientific Tables: Biochemistry, Metabolism of Xenobiotics, Inborn Errors of Metabolism, and Pharmacogenetics and Ecogenetics* (Ciba-Geigy, West Caldwell, NJ), Vol. 4, 8th Ed., p. 87.
32. Schmidt-Nielsen, K. (1990) in *Animal Physiology* (Cambridge Univ. Press, Cambridge), 4th Ed., pp. 193–194.
33. Curtis, S. E., Vallet, B., Winn, M. J., Caufield, J. B., King, C. Z., Chapler, C. K. & Cain, S. M. (1995) *J. Appl. Physiol.* **79,** 1351–1360.
34. Buerk, D. G. & Goldstick, T. K. (1982) *Am. J. Physiol.* **243,** H948–H958.
35. Bruttig, S. P. & Joyner, W. L. (1983) *J. Cell. Physiol.* **116,** 173–180.
36. Oldendorf, W. H., Cornford, M. E. & Jann Brown, W. (1977) *Ann. Neurol.* **1,** 409–417.
37. Seccombe, J. F. & Schaff, H. V. (1994) *Vasoactive Factors Produced by the Endothelium: Physiology and Surgical Implications* (CRC, Boca Raton, FL).
38. Cain, B. S., Meldrum, D. R., Selzman, C. H., Cleveland, J. C., Meng, X., Sheridan, B. C., Banerjee, A. & Harken, A. H. (1997) *Surgery* **122**, 516–526.
39. Ryan, U. S. & Rubanyi, G. M. (1992) *Endothelial Regulation of Vascular Tone* (Dekker, New York).
40. Luscher, T. L. (1995) *The Endothelium in Cardiovascular Disease: Pathophysiology, Clinical Presentation, and Pharmacotherapy* (Springer, New York).
41. Davies, M. G. & Tripathi, S. C. (1993) *Ann. Surg.* **218,** 593–609.
42. Boswell, C. A., Majno, G., Joris, I. & Ostrom, K. A. (1992) *Microvasc. Res.* **43,** 178–191.
43. Gotlieb, A. I. & Wong, M. K. K. (1988) in *Endothelial Cells*, ed. Ryan, U. S. (CRC, Boca Raton, FL), pp. 31–101.
44. Yaegashi, K., Itoh, T., Kosaka, T., Fukushima, H. & Morimoto, T. (1996) *Am. J. Physiol.* **270,** H1390–H1397.